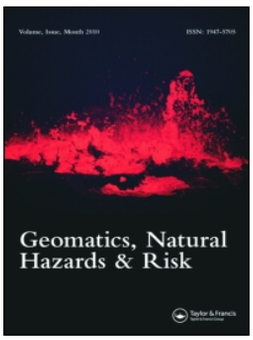

Geomatics, Natural Hazards and Risk

ISSN: 1947-5705 (Print) 1947-5713 (Online) Journal homepage: https://www.tandfonline.com/loi/tgnh20

First insights on the potential of Sentinel-1 for landslides detection

Anna Barra, Oriol Monserrat, Paolo Mazzanti, Carlo Esposito, Michele Crosetto & Gabriele Scarascia Mugnozza

To cite this article: Anna Barra, Oriol Monserrat, Paolo Mazzanti, Carlo Esposito, Michele Crosetto & Gabriele Scarascia Mugnozza (2016) First insights on the potential of Sentinel-1 for landslides detection, Geomatics, Natural Hazards and Risk, 7:6, 1874-1883, DOI: 10.1080/19475705.2016.1171258

To link to this article: https://doi.org/10.1080/19475705.2016.1171258

Published online: 03 May 2016.

GEOMATICS, NATURAL HAZARDS AND RISK, 2016
VOL. 7, NO. 6, 1874–1883
http://dx.doi.org/10.1080/19475705.2016.1171258

Taylor & Francis
Taylor & Francis Group

OPEN ACCESS

First insights on the potential of Sentinel-1 for landslides detection

Anna Barra[a], Oriol Monserrat[a], Paolo Mazzanti[b,c], Carlo Esposito[b], Michele Crosetto[a] and Gabriele Scarascia Mugnozza[b,c]

[a]Centre Tecnològic de Telecomunicacions de Catalunya (CTTC), Division of Geomatics, Castelldefels, Barcelona, Spain; [b]Dipartimento di Scienze della Terra, Università degli Studi di Roma 'La Sapienza', Rome, Italy; [c]NHAZCA S.r.l., spin off Università degli Studi di Roma 'La Sapienza', Rome, Italy

ABSTRACT

This paper illustrates the potential of Sentinel-1 for landslide detection, mapping and characterization with the aim of updating inventory maps and monitoring landslide activity. The study area is located in Molise, one of the smallest regions of Italy, where landslide processes are frequent. The results achieved by integrating Differential Synthetic Aperture Radar Interferometry (DInSAR) deformation maps and time series, and Geographical Information System (GIS) multilayer analysis (optical, geological, geomorphological, etc.) are shown. The adopted methodology is described followed by an analysis of future perspectives. Sixty-two landslides have been detected, thus allowing the updating of pre-existing landslide inventory maps. The results of our ongoing research show that Sentinel-1 might represent a significant improvement in terms of exploitation of SAR data for landslide mapping and monitoring due to both the shorter revisit time (up to 6 days in the close future) and the wavelength used, which determine an higher coherence compared to other SAR sensors.

ARTICLE HISTORY
Received 28 October 2015
Accepted 23 March 2016

KEYWORDS:
InSAR; Sentinel-1; landslide inventory map; landslide activity; monitoring

1. Introduction

A precise inventory map containing information on landslide activity is an essential input to landslide susceptibility and hazard analyses. The contribution of satellite Synthetic Aperture Radar (SAR) interferometry to landslide risk mitigation is well known within the scientific community and many encouraging results have been obtained (Catani et al. 2005; Herrera et al. 2009; Righini et al. 2012; Cigna et al. 2013; Crosetto et al. 2013; Raspini et al. 2013; Frangioni et al. 2014; Ciampalini et al. 2015; Rocca et al. 2015). Areas characterized by high coherence of images (e.g. due to rock lithology or urban setting) are required to obtain results and, in this regard, the expected increased capabilities of Sentinel-1, compared to other SAR sensors such as ERS, ENVISAT or ALOS, for landslide mapping and monitoring are related to both the wavelength (55.5 mm) and the short temporal baseline (12 days) (Ferretti et al. 2007). The latter is expected to be a key feature for enhanced coherence and, therefore, to define monitoring and updating plans. A set of 14 Sentinel-1 images acquired over the Molise region, Southern Italy (Figure 1), a critical area geologically susceptible to landslides, were processed with the aim of assessing these potentialities. Even though the Molise region is mostly covered by agricultural fields and forests (63% and 35%, respectively; Di Somma 2011),

CONTACT Anna Barra anna.barra@cttc.cat

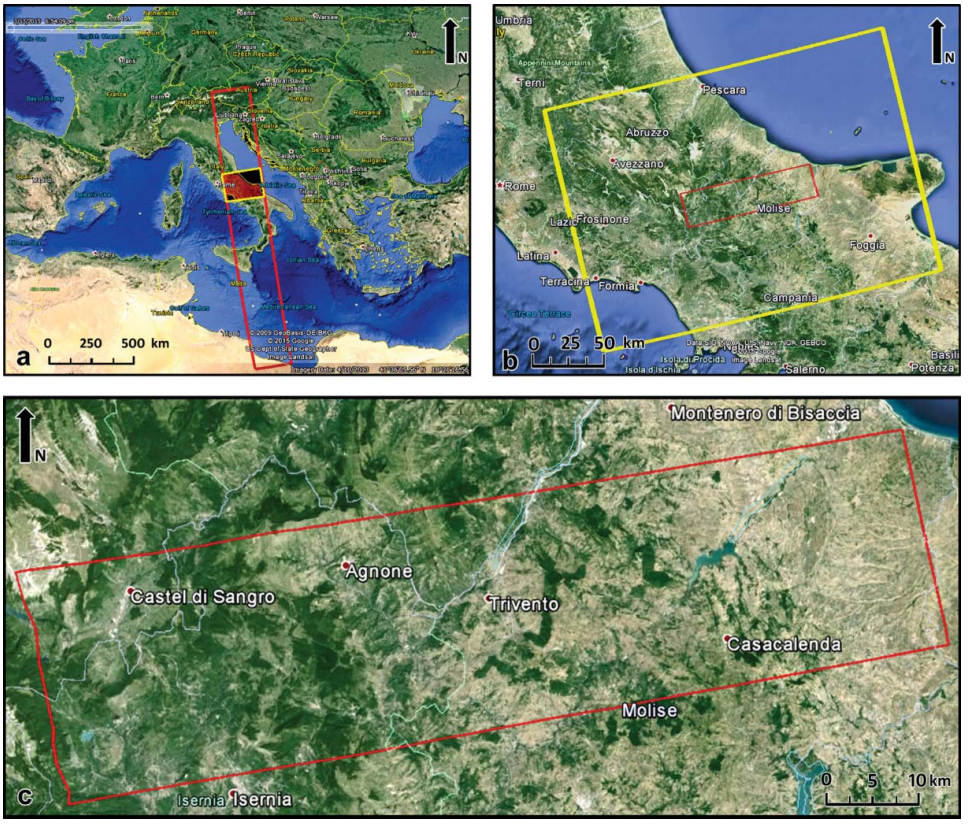

Figure 1. (a) The Sentinel-1 strip and the selected frame (ESA); (b) zoom of the selected frame and location of the analyzed area, corresponding to a single burst; (c) zoom of the analyzed area.

indicating non-optimal conditions for SAR coherence, promising results have been obtained by spatially and temporally examining 12-days interferograms followed by a multilayer analysis in a Geographical Information System (GIS) environment.

2. Study area: the Molise region

The Molise region is located in Southern Italy and is one of the Italian regions most affected by landslide phenomena (Rosskopf & Aucelli 2007). From the geo-lithological point of view (Molise Region 2001; Sgrosso & Naso 2012), Molise is composed by sedimentary formations: marine environment formations (from Triassic to Pleistocene) and recent continental deposits (Pliocene-Holocene). The study area (Figure 2) is mostly characterized by the turbidite sedimentation of Molisian Basin (Paleogene−Miocene), which includes the basal complex of 'Varicolor Clays' and flysches with different composition (marly-calcareous, marly-arenitic or mostly arenitic). A few zones, situated in the western part of the area, are characterized by calcareous-dolomitic lithologies of the carbonate platform (Piattaforma Abruzzese-Campana, Triassic−Cretaceous) and by calcareous-marl detrital sedimentation of the transitional ramp (Cretaceous−Miocene). The north-eastern area is characterized by the sandy-clayey deposits of the Adriatic Foredeep Basin (Pliocene−Pleistocene).

The geo-lithological and geomorphological settings make the Molise region prone to landslide movements. In fact, according to a recent study based on the Italian Inventory of Landslide Phenomena (IFFI) synthetized by Trigila et al. (2013), almost 18% of the Molise region is affected by landslides. The IFFI also classify as active about 67% of the identified landslides in Molise. The main

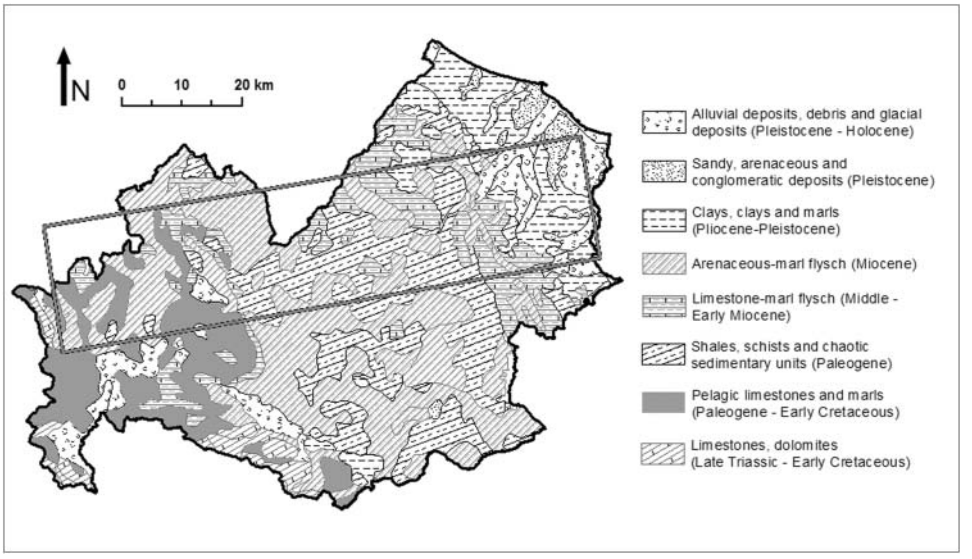

Figure 2. Lithologic map of the Molise region (scale 1:500,000). Data provided by the Institute for Environmental Protection and Research, ISPRA (Istituto Superiore per la Protezione e la Ricerca Ambientale).

landslide typologies are earth flows and complex movements (Figure 3) and are usually associated with the fluvial evolution (Aucelli et al. 2001) and triggered by intense rainfall events.

The study area was affected by several landslides (Figure 3(c,e)) during the analyzed period (October 2014−April 2015), mainly triggered by intense rainfalls occurred from December 2014 to March 2015 (Figures 5 and 6(c)).

3. Sentinel-1 data analysis

The Differential SAR Interferometry (DInSAR) procedure (Crosetto et al. 2011) used in this study (Figure 4) is explained in this section. Our investigation has focused on a single burst (Figure 1) of a set of 14 Sentinel-1 Interferometric Wide Swath images (single polarization VV) acquired in ascending orbit spanning the period November 2014−March 2015 (the acquisition dates of the images are shown in Figure 5(c)).

The procedure is divided into two main steps: the DInSAR analysis and the Multilayer GIS analysis. The first step is performed in SAR geometry and consists in the analysis of the interferometric data, both at spatial and temporal levels, with the aim of detecting areas affected by deformation and, therefore, characterizing landslide activity. The main output is a set of areas potentially affected by deformation. The second step (multilayer GIS analysis) consists in the integration of DInSAR derived data with geological and geomorphological data to interpret and validate the detected areas of deformation and, consequently, to update the pre-existing landslide inventory maps.

The steps of the procedure followed in this study (Figure 4) are:

- *Interferogram generation*: generation of the network of interferograms to be used in the analysis. Only interferometric pairs with the minimum temporal baseline (12 days, except one of 36 days) were estimated.
- *Spatial analysis*: visual inspection of the interferograms to identify spatial patterns with the potential to be deformation areas (Figures 5(b) and 6(a)) (Rocca et al. 2014). Note that this analysis only provides information on movements that are fast enough to be observed in 12 day periods. Once the patterns are detected, the pairwise logic (Massonnet & Feigl 1998) is

a	Typolgy	%
1	Earth flow	42
2	Complex	30
3	Rotational/translational	19
4	Debris flows	5
5	Superficial-widespread	3
6	Rock fall/toppling	1

Figure 3. (a) Percentage of landslide typologies in the Molise region (Rosskopf & Aucelli, 2007, Cruden & Varnes, 1996); (b) landslide of Ripalimosani (Campobasso), April 1996 (Rosskopf & Aucelli, 2007); (c) Google Earth satellite image showing landslides near Trivento city (acquisition date: 10 December 2014).

used to discard patterns attributable to other sources, such as topographic errors or atmosphere (Hanssen 2001). The result of this step is a set of areas potentially affected by deformation.

– *Temporal analysis (time series estimation)*: time series generation over a selected subset of pixels. The procedure involves unwrapping the interferograms (Costantini 1998) using only pixels with a coherence value higher than a given threshold (0.2 in this work). The temporal series are then obtained by integrating the unwrapped phases as follows:

$$\begin{cases} \varphi_j = \varphi_{j-1} + \Delta\varphi_{j(j-1)} \\ \varphi_0 = 0 \end{cases} \quad (1)$$

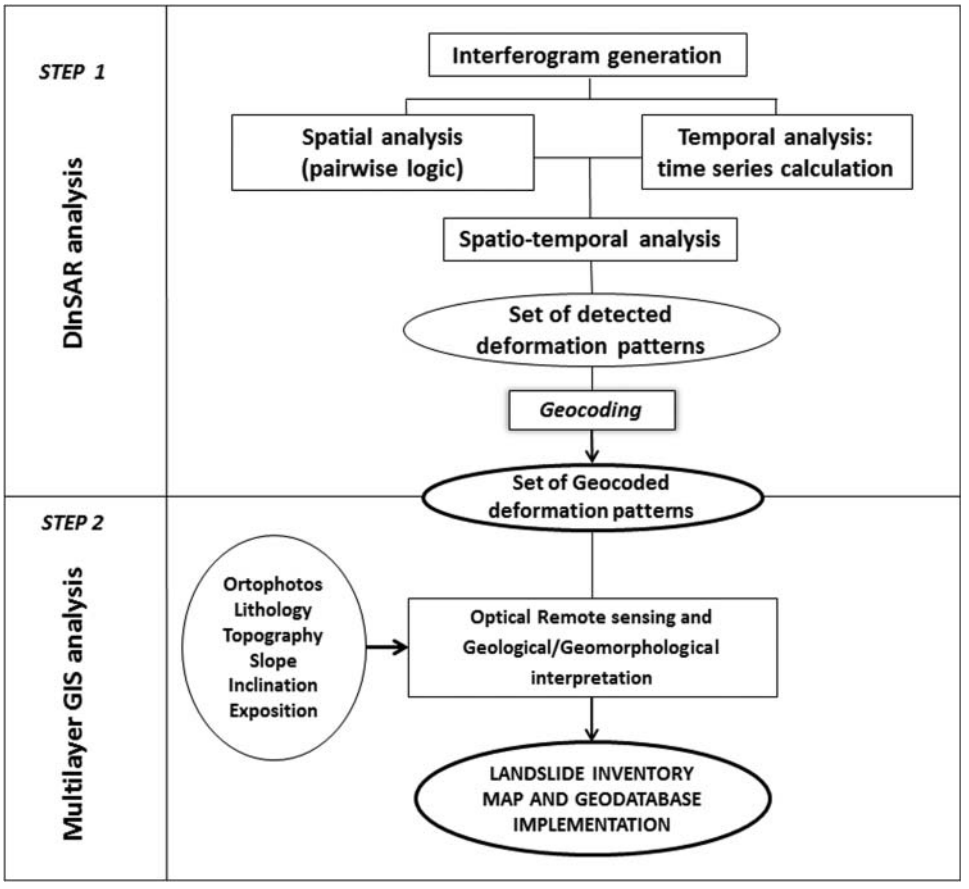

Figure 4. Flow-chart of the procedure used in this study.

where φ_j and φ_0 are the accumulated and the reference phases, and $\Delta\varphi_{j(j-1)}$ is the interferometric phase calculated from images $j-1$ and j. Thus, the temporal evolution of the phase is obtained for each point. Finally, the map of accumulated deformation is analyzed to search for new spatial patterns characterized by slow deformation rates (Figure 6(b)). It is worth underlining that the analysis of the time series is done with respect to a local stable reference to avoid critical atmospheric effects.

– *Spatio-temporal analysis*: the potential areas of deformation detected in the previous steps are analyzed together with the time series. This combined analysis is useful to: (i) detect phase unwrapping errors (aliasing); (ii) assess the temporal behaviour of each detected deformation phenomenon; (iii) confirm or modify the shape of the deformation area detected. The result of this step is the final set of detected deformation phenomena.

The first block ends with the georeferencing of the deformation phenomena to a known coordinate system.

– *Multilayer GIS analysis*: geological/geomorphological interpretation of the detected areas by the exploitation of different information layers in a GIS environment: Digital Elevation Model and derived data (e.g. aspect and slope), ortophoto interpretation, geo-lithological maps, existing landslide inventory maps, etc. The previously identified potential deformation areas are confirmed, denied or modified in this phase and the results can be used to update landslide inventory maps.

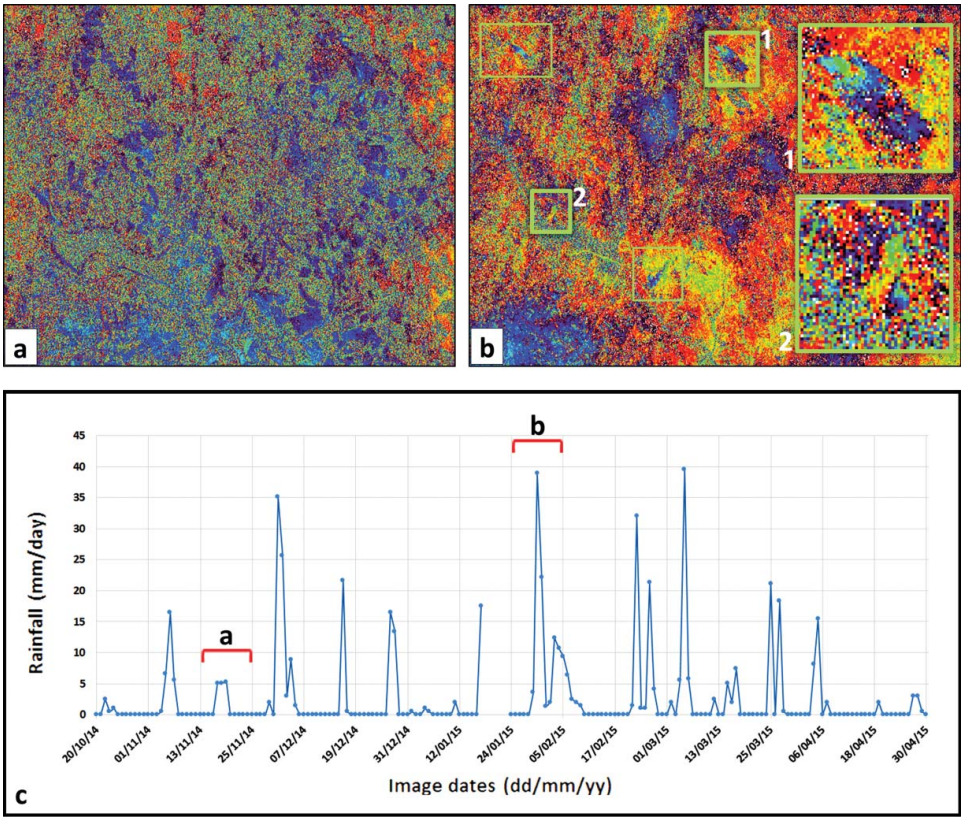

Figure 5. Interferograms derived from images collected on 13 November 2014 and 25 November 2014 (a) and on 24 January 2015 and 5 February 2015 (b). The rectangles in (b) highlight several potential deformation phenomena and two of them are zoomed (squares 1 and 2); (c) daily rainfall during the analyzed period, where the a and b letters mark the periods of the interferograms from (a) and (b). (b) shows more deformation patterns than (a), which is coherent with the higher precipitation amount of the related period.

4. Achieved results

The potential deformation phenomena detected during the interferometric analysis (Figure 5) are mostly concentrated in the interferograms including high precipitation periods. This is a promising result since intense rainfall is the main triggering/accelerating factor of the studied landslides.

Figure 6 displays an example of landslide detected in an interferogram that clearly shows the shape of the deformation area. Figure 6(b) shows the same area in the accumulated deformation map, where the colours represent the deformation in line of sight (LOS) because SAR sensors can only measure the projection of the real movement along the LOS. Two deformation areas with opposite sign (the red and the blue one) are displayed. This is the effect of the combination between landslide movement and radar LOS direction (see Figure 6(d)): in the blue area the main slope inclination is toward the satellite (SW direction), while in the red one it is outward (E−SE direction). Furthermore, the central area appears to suffer smaller displacements because the main direction of the deformation is almost parallel to LOS, which is not detectable with this technique. The shape of the landslide area is better bounded by jointly analyzing the interferogram and the accumulated deformation map. Aliasing errors can be checked at the time series (Figure 6(c)) by analyzing the consistency with the displacement information of the interferogram. Furthermore, Figure 6(c) shows how the time series analysis allowed characterizing the temporal activity of the landslide, even when the deformation is not fast enough to be well observed in a 12-day interferogram. The

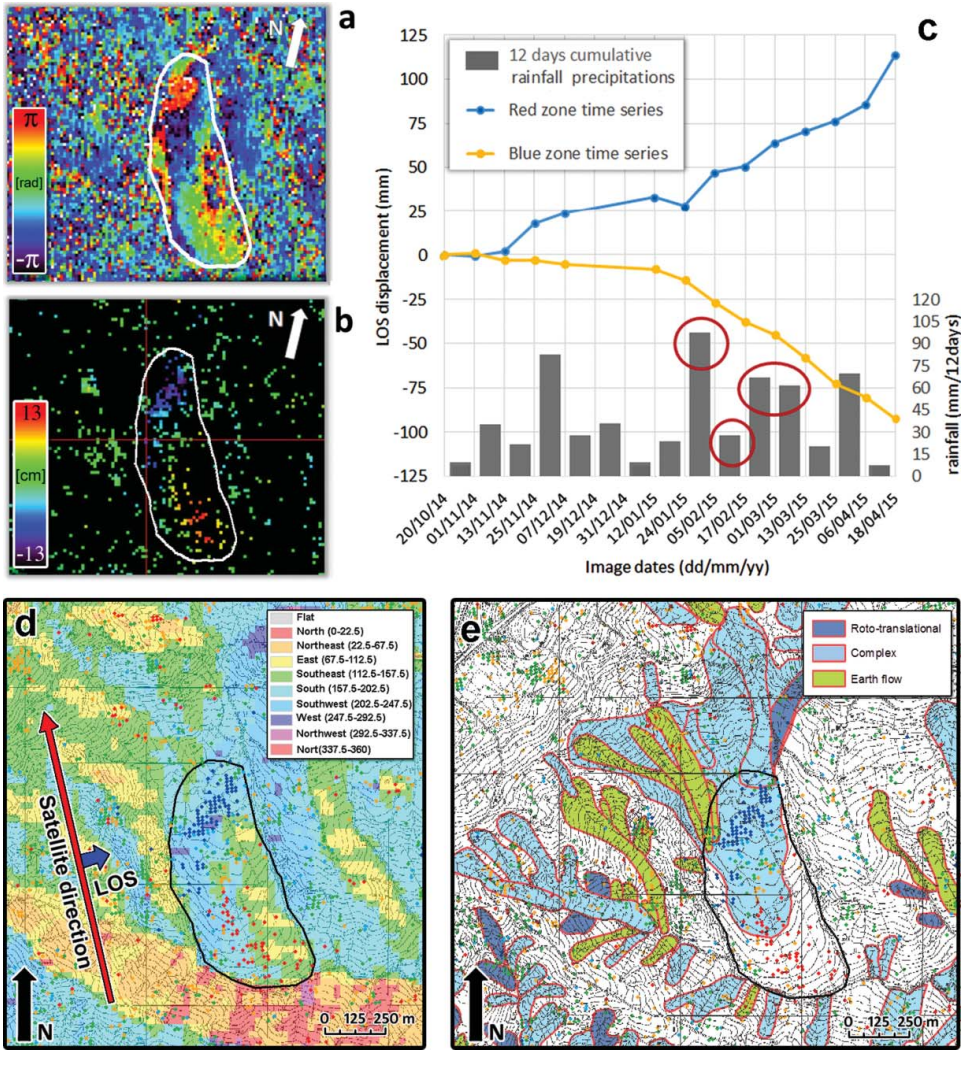

Figure 6. (a) Potential deformation phenomenon in the 12-day interferogram covering the period from 24 January 2015 to 5 February 2015; (b) the same deformation pattern in the total accumulated deformation map (over the selected subset of pixels). Two main areas can be distinguished: the red one and the blue one; (c) time series in line of sight (LOS) of the two areas (blue and red) and 12-day cumulative rainfall corresponding to each interferogram. Red circles indicate the periods when the interferograms clearly show the deformation pattern; (d) and (e) the accumulated deformation map (coloured points) superimposed to a topographic base-map. The black polygon represents the detected deformation area. In (d) is also showed the slope exposition map and the satellite and LOS directions; in (e) the coloured polygons are the landslides of the Italian Landslide Phenomena Inventory (IFFI). Note that the colour scale of the points in (d) and (e) is the same of figure (b).

retrieved deformation pattern allowed a better definition of the boundary and the activity of an existing landslide (Figure 6(e)).

A set of 29 potential deformation phenomena were detected during the DInSAR analysis (Figure 4), which were then georeferenced and integrated with other information layers in the GIS analysis that confirmed the areas to be affected by landslides. Moreover, in some cases, the analysis of a single detected deformation area allowed to distinguish different landslide bodies (Figure 7). Table 1 summarizes the results obtained compared with the existing inventory: a total of 62 active landslides were detected of which 13 are new, 31 have been updated in terms of spatial delimitation and 18 have been confirmed to be active.

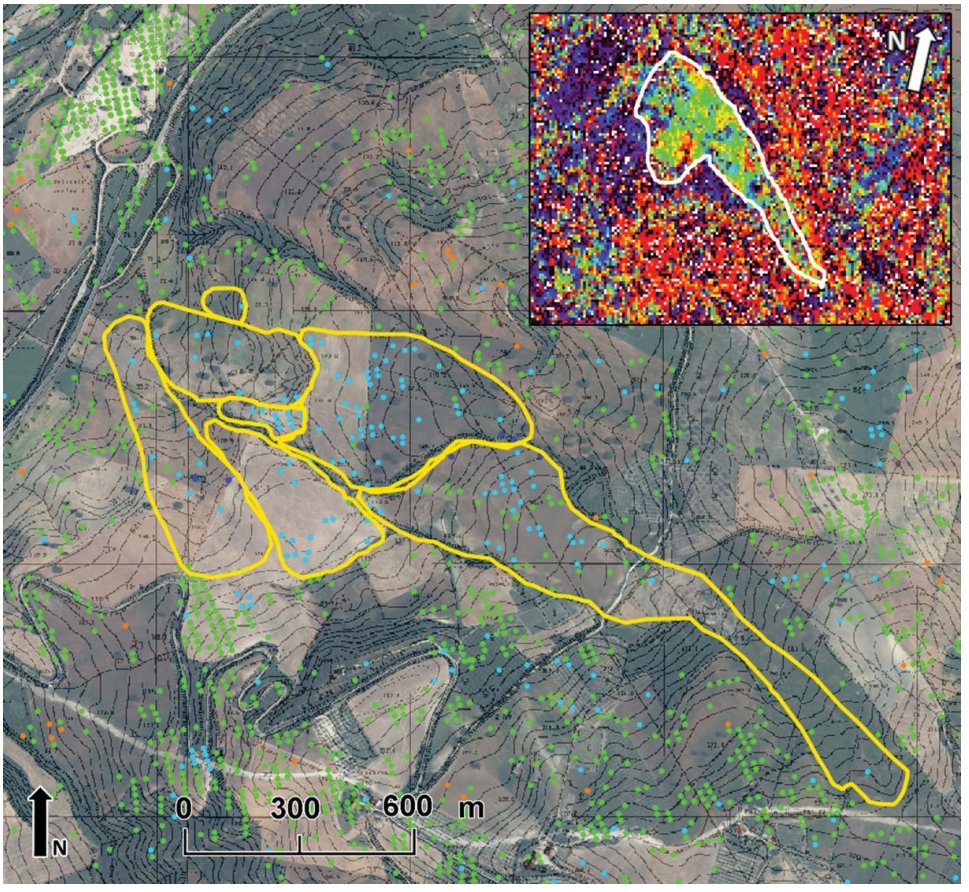

Figure 7. Example of landslide bodies distinguished during the multilayer GIS analysis step are shown in this figure, that also displays the accumulated deformation map (coloured points) superimposed on a topographic base. The image at the upper-right shows the deformation pattern (bounded by a white line) detected in an interferogram.

Table 1. Detected potential deformation phenomena and confirmed landslides.

	Detected deformation patterns	Landslide polygons	Comparison with the existing inventory		
			NEW	UPDATED	CONFIRMED
Abs. Number	29	62	13	31	18

5. Conclusions and outlook

The research carried out in this work is aimed at evaluating the performance of Sentinel-1 data for landslide mapping and monitoring. Fourteen Sentinel-1 SLC images, acquired during a temporal span of seven months in the Molise region (Italy), have been processed. A single burst of a Sentinel-1 frame (approximately 1875 km^2) has been analyzed by integrating DInSAR techniques with geological/geomorphological data in a multilayer GIS environment.

Despite the short period of time and, therefore, the small number of images available, 62 active landslides have been detected, thus allowing updating the pre-existing inventory maps both in terms of landslide boundaries and activity. These results demonstrate the potential of Sentinel-1 for landslide analysis and monitoring. Besides, a better understanding of landslide behaviour and its relationship with the triggering factors is expected when longer Sentinel-1 time series are available for analysis. This will be a key issue to perform hazard analyses.

The main disadvantage of the procedure used in this study is the manual data analysis and interpretation which makes the analysis cumbersome and operator-dependent. In this regard, further research will be focused on developing algorithms to automatically detect and extract patterns in the interferograms and rules to ease the GIS analysis. This will be done by integrating Sentinel-1 data and other types of data, in particular Sentinel-2 imagery.

Acknowledgments

This research has been partially funded by the European Commission, Directorate-General Humanitarian Aid and Civil Protection (ECHO), through the SAFETY project (Ref. ECHO/SUB/2015/718679/Prev02) and by the Spanish Ministry of Economy and Competitiveness through the project MIDES (Ref:CGL2013-43000-P).

Disclosure statement

No potential conflict of interest was reported by the authors.

References

Aucelli PP, Cinque A, Rosskopf C. 2001. Geomorphological map of the Trigno basin (Italy): explanatory notes. Geogr Fis Din Quat. 24:3−12.

Catani F, Casagli N, Ermini L, Righini G, Menduni G. 2005. Landslide hazard and risk mapping at catchment scale in the Arno River basin. Landslides. 2:329−342.

Ciampalini A, Raspini F, Bianchini S, Frodella W, Bardi F, Lagomarsino D, Di Traglia F, Moretti S, Proietti C, Pagliara P, et al. 2015. Remote sensing as tool for development of landslide databases: the case of the Messina Province (Italy) geodatabase. Geomorphology. 249:103−118.

Cigna F, Bianchini S, Casagli N. 2013. How to assess landslide activity and intensity with Persistent Scatterer Interferometry (PSI): the PSI-based matrix approach. Landslides. 10:267−283.

Crosetto M, Gili JA, Monserrat O, Cuevas-González M, Corominas J, Serral D. 2013. Interferometric SAR monitoring of the Vallcebre landslide (Spain) using corner reflectors. Nat Hazard Earth Syst Sci. 13:923−933.

Crosetto M, Monserrat O, Cuevas M, Crippa B. 2011. Spaceborne differential SAR interferometry: data analysis tools for deformation measurement. Remote Sens. 3:305−318.

Costantini M. 1998. A novel phase unwrapping method based on network programming. IEEE Trans Geosci Remote Sens. 36:813−821.

Cruden DM, Varnes DJ. 1996. Landslide types and processes. In: Special Report 247 – Landslides: Investigation and mitigation. Washington DC: Transportation Research Board.

Di Somma A. 2011. L'uso del suolo agrario d'Italia. Roma: VALMAR. Italian.

Ferretti A, Monti-Guarnieri A, Prati C, Rocca F, Massonet D. 2007. InSAR Principles-Guidelines for SAR Interferometry Processing and Interpretation, 19. The Netherlands: Esa Publications.

Frangioni S, Bianchini S, Moretti S. 2014. Landslide inventory updating by means of persistent scatterer interferometry (PSI): The Setta basin (Italy) case study. Geomat Nat Hazard Risk. 6:419−438.

Hanssen RF. 2001. Radar interferometry: data interpretation and error analysis. The Netherlands: Kluwer Academic Publishers.

Herrera G, Davalillo JC, Mulas J, Cooksley G, Monserrat O, Pancioli V. 2009. Mapping and monitoring geomorphological processes in mountainous areas using PSI data: Central Pyrenees case study. Nat Hazard Earth Syst Sci. 9:1587−1598.

Massonnet D, Feigl KL. 1998. Radar interferometry and its application to changes in the Earth's surface. Rev Geophys. 36:441−500.

Meteoweb. 2015. Available from: http://www.meteoweb.eu/2015/02/maltempo-situazione-critica-in-molise-evacuazioni-strade-interrotte-trivento-bojano/402570/. Italian.

Molise Region. 2001. Mitigazione del rischio sismico dei centri storici e degli edifici di culto dell'area del Matese nella Regione Molise. [Seismic risk mitigation in the historic centers and religious buildings in the Matese area of Molise region]. Gruppo Nazionale per la Difesa dai Terremoti, Istituto Nazionale di Geofisica e Vulcanologia, Italy. Italian.

Raspini F, Moretti S, Casagli N. 2013. Landslide mapping using SqueeSAR data: Giampilieri (Italy) case study. In Landslide science and practice. Berlin Heidelberg: Springer-Verlag; p. 147−154.

Righini G, Pancioli V, Casagli N. 2012. Updating landslide inventory maps using Persistent Scatterer Interferometry (PSI). Int J Remote Sens. 33:2068−2096.

Rocca A, Mazzanti P, Perissin D, Bozzano F. 2014. Detection of past slope activity in a desert area using multi-temporal DInSAR with ALOS PALSAR data. Ital J Eng Geol Environ; p. 35–49. Italy.

Rocca A, Mazzanti P, Bozzano F, Perissin D. 2015. Advanced characterization of a landslide-prone area by satellite a-DInSAR. In: Engineering geology for society and territory, Volume 5. Switzerland: Springer International Publishing; p. 177–181

Rosskopf CM, Aucelli PPC. 2007. Analisi del dissesto da frana in Molise. In: Rapporto sulle frane in Italia - Il Progetto IFFI - Metodologia, Risultati e rapporti regionali, APAT [Analysis of landslide instabilities in Molise]. In: Report on landslides in Italy – The IFFI Project – Methodology, results and regional reports, APAT; p. 493–508, Cap. 19. Italian.

Sgrosso I, Naso G. 2012 Note illustrative della Carta Geologica d'Italia in scala 1:50.000, Foglio n. 393, Trivento. [Notes of the Geological Map of Italy at scale 1 : 50,000, sheet no. 393, Trivento]. Roma: Servizio Geologico d'Italia (ISPRA). Italian.

Trigila A, Frattini P, Casagli N, Catani F, Crosta G, Esposito C, Iadanza C, Lagomarsino D, Lari S, Scarascia-Mugnozza G, et al. 2013. Landslide susceptibility mapping at national scale: the Italian case study. In Landslide science and practice. Inventory and hazard assessment. Berlin Heidelberg: Springer-Verlag; Vol. 1, p. 287–296.